Generation of humanized mouse models to support therapeutic development for SYNGAP1 and STXBP1 disorders

Alex J. Felix[1,2], Taryn Wilson[1,2], Rani Randell[1,2], Nicolas Marotta[1,2,3], Keita Uchida[1], Michael J. Boland[2], Beverly L. Davidson[2,4,5] and Benjamin L. Prosser[1,2*].

[1]Department of Physiology, University of Pennsylvania Perelman School of Medicine, Philadelphia, PA 19104, USA.

[2]Center for Epilepsy and Neurodevelopmental Disorders (ENDD), University of Pennsylvania Perelman School of Medicine and Children's Hospital of Philadelphia, Philadelphia, PA 19104, USA.

[3]Biochemistry and Molecular Biophysics Graduate group, University of Pennsylvania Perelman School of Medicine, Philadelphia, PA 19104, USA.

[4]Center for Cellular and Molecular Therapeutics, Children's Hospital of Philadelphia, Philadelphia, PA 19104, USA.

[5]Department of Pathology and Laboratory Medicine, University of Pennsylvania Perelman School of Medicine, Philadelphia, PA 19104, USA.

*to whom correspondence should be addressed:

*Benjamin L. Prosser – bpros@pennmedicine.upenn.edu

Key words: SYNGAP1, STXBP1, epileptic encephalopathy, humanized mouse model, gene-targeted therapies.

Author emails:

Alex J. Felix: Alejandro.JimenezFelix@Pennmedicine.upenn.edu

Taryn Wilson: taryn.wilson@pennmedicine.upenn.edu

Rani Randell: rrani@sas.upenn.edu

Nicolas Marotta: nick.marotta@pennmedicine.upenn.edu

Keita Uchida: keita.uchida@pennmedicine.upenn.edu

Michael J. Boland: michael.boland@pennmedicine.upenn.edu

Beverly L. Davidson: davidsonbl@chop.edu

Acknowledgements

We thank Elizabeth A. Heller (University of Pennsylvania) for assisting with the design of the humanized mouse models. We thank Jennine M. Dawicki-McKenna (University of Pennsylvania) for providing feedback on the manuscript.

Funding information

This work was supported by R21 NS118280 from NIH-NINDS to B.L.P. and B.L.D.

Conflicts of interest

BLP and BLD are inventors on two patents relevant to therapeutic development for neurodevelopmental disorders, PCT/US2020/031672 and UPN-22-9943. AJF is an inventor on UPN-22-9943.

Data availability statement

The data that support the findings of this study are available from the corresponding author upon reasonable request.

Author contributions

A.J.F., M.J.B., B.L.D and B.L.P. contributed to experimental design. A.J.F., T.W., R.R. and N.M. performed the experiments and collected the data. K.U. maintained and expanded the mouse colonies. Writing original draft: A.J.F. Writing - Review & Editing: B.L.P. and A.J.F. Funding acquisition: B.L.P. All authors approved the final manuscript.

Abstract

Heterozygous variants in *SYNGAP1* and *STXBP1* lead to distinct neurodevelopmental disorders caused by haploinsufficient levels of post-synaptic SYNGAP1 and pre-synaptic STXBP1, which are critical for normal synaptic function. While several gene-targeted therapeutic approaches have proven efficacious *in vitro*, these often target regions of the human gene that are not conserved in rodents, hindering the pre-clinical development of these compounds and their transition to the clinic. To overcome this limitation, here we generate and characterize *Syngap1* and *Stxbp1* humanized mouse models in which we replaced the mouse *Syngap1* and *Stxbp1* gene, respectively, with the human counterpart, including regulatory and non-coding regions. Fully humanized *Syngap1* mice present normal viability and can be successfully crossed with currently available *Syngap1* haploinsufficiency mouse models to generate *Syngap1* humanized haploinsufficient mice. *Stxbp1* mice were successfully humanized, yet exhibit impaired viability (particularly males) and reduced STXBP1 protein abundance. Mouse viability could be improved by outcrossing this model to other mouse strains, while *Stxbp1* humanized females and hybrid mice can be used to evaluate target engagement of human-specific therapeutics. Overall, these humanized mouse models represent a broadly available tool to further pre-clinical therapeutic development for SYNGAP1 and STXBP1 disorders.

Introduction

De novo, heterozygous mutations in *SYNGAP1* and *STXBP1* lead to distinct, rare neurodevelopmental disorders (NDDs) with an incidence of ~1 in 10,000 and ~1 in 30,000 births, respectively (1). Mutations often lead to haploinsufficient levels of post-synaptic Synaptic Ras GTPase Activating Protein 1 (SYNGAP1) and pre-synaptic Syntaxin Binding Protein 1 (STXBP1), which are each critical for proper synaptic function and plasticity (2,3). SYNGAP1 and STXBP1 epileptic encephalopathies are characterized by severe-to-profound intellectual disability, epilepsy, motor dysfunction and autistic features (4–6). No treatments currently exist that alter the course of these disorders nor that address the underlying pathomechanism.

Several therapeutic modalities to rescue haploinsufficiency are in development for these disorders, including antisense oligonucleotide approaches (7–9), engineered translational activators (10,11), and CRISPR activation strategies, among others. Several approaches have already proven efficacious at restoring target gene levels in *in vitro* systems, including Induced Pluripotent Stem Cell-derived neurons from STXBP1 or SYNGAP1 patients. Yet many of these candidate therapies target specific regions of the human gene sequence that are not fully conserved in rodent species and are thus incompatible for *in vivo* testing in current mouse models (*Syngap1*$^{+/-}$ or *Stxbp1*$^{+/-}$) (12,13). This highlights the need to generate new animal models that incorporate the molecular features of the target human gene, enabling assessments of *in vivo* efficacy of human gene targeted approaches to accelerate their transition to the clinic.

Towards this goal, here we report the generation and characterization of *Syngap1* and *Stxbp1* humanized mouse models. The humanization process excised the entire *Syngap1* or *Stxbp1* locus from the mouse genome and incorporated the respective human gene, including upstream and downstream regulatory regions, to allow broad utility for different gene-targeted approaches.

Materials and Methods

Generation of *Syngap1* and *Stxbp1* humanized mouse models

The *Syngap1* humanized mouse model is a non-conditional knock-in (KI) model generated by introducing a ~37.5 kb of gDNA encoding the human *SYNGAP1* and *ZBTB9* genes in place of a ~34.7 kb of the murine *Syngap1* and *Zbtb9* genes (**Figure 1A**) via Bacterial Artificial Chromosome (BAC) targeting in mouse Embryonic Stem (ES) cells. The entire *Syngap1* locus is humanized (including promoter, proximal enhancers, 5'UTR, coding sequence, intronic regions and the entire 3'UTR), while the *Zbtb9* is only humanized up to the STOP codon (**Figure 1A, magenta box**). This allows for the inclusion of the *SYNGAP1* antisense transcript (*SYNGAP1-AS*) within the humanized region (**Figure 1A, orange box**), to enable testing of therapeutic approaches targeting this element. The final KI human gDNA was flanked with loxP sites.

The humanization of *Syngap1* may affect the expression of the *Cuta* gene (**Figure 1A, brown boxes**) since the *Syngap1* and *Cuta* genes appear to share a divergently transcribed promoter and approximately half of the region corresponding to this promoter was humanized.

The Stxbp1 humanized mouse model is a non-conditional KI model also generated by BAC targeting in mouse ES cells. The BAC replaced the murine genomic region from approximately 5.4 kb upstream of *Stxbp1* exon 1 through to near the end of exon 19 with the human genomic region from approximately 4.0 kb upstream of *STXBP1* exon 1 (Transcript ENST00000373299) through to the end of the final exon of human *STXBP1* transcript ENST00000636962. This represents the introduction of ~89 kb of gDNA encoding the human *STXBP1* (including promoter, proximal enhancers, 5'UTR, coding sequence, intronic regions and the entire 3'UTR) in place of ~66Kb of the murine *Stxbp1*. The final KI human gDNA was flanked with loxP sites. The humanized region may express the miR-3911 (**Figure 2A, red box**) and lncRNA ENST00000624141 (**Figure 2A, yellow box**), as well as the short 35 residue isoform of PTRH1 (Uniprot: A0A286YER0) (**Figure 2A, orange boxes**).

All mouse gene engineering steps were performed by Ozgene. The BAC constructs for *Syngap1* and *Stxbp1* humanization were constructed by a third-party who validated its correctness by restriction digestion and Pulse-Field Gel Electrophoresis. Inserted cassettes and additional modified parts of the BACs were confirmed by PCR and sequencing. Ozgene also performed independent quality controls by sequencing or qPCR of key regions such as loxP sites, neomycin and hygromycin cassettes, junctions, and presence of *SYNGAP1* and *STXBP1* transgenes. The BACs were electroporated into C57BL/6 ES cells and qPCR assays were carried out to confirm correct targeting as well as presence of the selection cassettes and the corresponding inserts. Gene-targeted ES cell clones were injected into goGermline blastocysts to produce goGermline chimeras followed by F1 heterozygous targeted mice (Hu/+) in which the selection cassettes (neomycin and hygromycin) were removed by mating the chimeras to a ubiquitous Flp line.

The resulting *Syngap1* and *Stxbp1* humanized mouse models are made available through JAX under MMRRC_069939 and MMRRC_071410, respectively.

Animals

The *Syngap1* humanized mouse model was maintained on a pure C57BL/6J genetic background, while the *Stxbp1* humanized model was maintained on a mixed genetic background of C57BL/6J outcrossed one generation to the BALB/c strain. Both male and female mice were used in this study. All animals were housed in the University of Pennsylvania Perelman School of Medicine animal facility in accordance with the standards set forth by the University of Pennsylvania Institutional Animal Care and Use Committee and the Guide for the Care and Use of Laboratory Animals published by the US National Institutes of Health under protocol #807524. Mice were maintained on a 12:12-h light:dark cycle and had *ad libitum* access to food and water throughout the experiments.

Mice were weaned at the age of 21 days and body weight measurements were obtained twice per week until animals reached 12 weeks of age. Survivability was assessed up to 36 weeks of age.

Copy number variation assay

Ear samples or tail snips from mice were collected in 1.5 mL tubes for genotyping. Genomic DNA (gDNA) extraction was performed by adding 100 µL of DirectPCR Lysis Reagent (Viagen Biotech #402-E) supplemented with proteinase K (Viagen Biotech #505-PKP) and incubating the samples at 56 °C overnight. Proteinase K was then inactivated at 86 °C for 45 min and samples were centrifuged at 8,000 x g for 1 min. The supernatant containing gDNA was directly used for qPCR-based genotyping or stored at 4 °C.

The copy number variation assay with qPCR was prepared by mixing the following reagents: 1 µL of crude gDNA, 1X PrimeTime Gene Expression Master Mix (IDT #1055772), 1X primers/probe mix and nuclease-free water to a final volume of 10 µL. Three technical replicates were performed for each sample. qPCR was carried out on a QuantStudio 3 Real-Time PCR System (ThermoFisher) with a passive reference of ROX using the following cycling conditions: 95 ºC for 3 min for 1 cycle, 95 ºC for 15 s and 62 ºC for 1 min for 40 cycles. ΔCt was calculated by subtracting the average Ct of the reference gene from the average Ct of the gene of interest for each sample. ΔΔCt values were obtained by subtracting the average ΔCt value of the control sample from the ΔCt of the test samples, and then converted into $2^{-\Delta\Delta Ct}$ to obtain the fold change of gene expression. Mouse *Tert* was used as endogenous control. In all reactions, samples from WT animals (+/+) were included to determine a reference Ct value corresponding to the presence of two copies of the mouse allele.

RNA isolation and RT-qPCR

Total RNA from mouse brain tissue was extracted using TRIzol. Tissue section (~1/4 of a cortex) was mixed with 1 mL of TRIzol reagent (Invitrogen #15596018) and a 5 mm stainless steel bead (Qiagen #69989) in an RNase-free microcentrifuge tube. Brain tissue was then homogenized in a TissueLyser LT homogenizer (Qiagen #85600) for 5 min at 50 Hz. The homogenate was centrifuge at 12,000 x g for 5 min at 4 °C and then seated for an additional 5 min to precipitate insoluble debris. The supernatant was transferred to a new tube, mixed with 200 µL of chloroform (Acros Organics #190764), shaken vigorously and centrifuged at 12,000 x g for 15 min at 4 °C. Aqueous phase was transferred to a new tube containing 500 µL of ice-cold isopropanol (Sigma-Aldrich #190764) followed by incubation for 10 min on ice and centrifugation at 12,000 x g for 10 min at 4 °C to precipitate RNA. Supernatant was discarded and 1 mL of ice-cold 75% ethanol (Decon laboratories #2701) was added to wash the pellet followed by centrifugation at 7,500 x g for 5 min at 4 °C. Supernatant was again discarded and RNA pellet was air-dried for 20 min. RNA was resuspended in 100 µL of RNase-free water and allowed to reconstitute for 10 min at 56 °C. To ensure RNA integrity for downstream applications, the resuspended RNA was purified using the Quick RNA Miniprep kit (Zymo #R1055) following manufacturer's instructions. Purified RNA was resuspended in 50 µL of RNase-free water. RNA concentration was determined by measuring OD_{260} nm absorbance in a Synergy HTX reader (Biotek).

cDNA synthesis was performed using the SuperScript IV First-Strand Synthesis System with ezDNase Enzyme (ThermoScientific #18091300) using random hexamer primers according to manufacturer's instructions. The ezDNase treatment step was performed for all conditions.

Probe-based qPCR was prepared by mixing the following reagents: 1 µL of cDNA, 1X PrimeTime Gene Expression Master Mix (IDT #1055772), 1X primers/probe mix and nuclease-free water to a final volume of 10 µL. Three technical replicates were performed for each sample. qPCR was carried out on a QuantStudio 3 Real-Time PCR System (ThermoFisher) with a passive reference of ROX using the following cycling conditions: 95 ºC for 3 min for 1 cycle, 95 ºC for 5 s and 60 ºC for 30 s for 40 cycles. ΔCt was calculated by subtracting the average Ct of the reference gene from the average Ct of the gene of interest for each sample. ΔΔCt values were obtained by subtracting the average ΔCt value of control samples from the ΔCt of the test samples, and then converted into $2^{-\Delta\Delta Ct}$ to obtain the fold change of gene expression.

All qPCR primer probe sets sequences can be found in **Table 1**.

Protein isolation and Western blot

Tissue section (~1/4 of a cortex) was mixed with 500 uL of 1.5x Laemmli buffer [15% glycerol (Amresco #M152), 3% SDS (Sigma #L5750), 3.75 mM EDTA (Bio-Rad #1610729) and 75 mM Tris, pH 7.5 (Invitrogen #15567027)] in a 2 mL sample tube (Qiagen #990381) and a 5 mm stainless steel bead (Qiagen #69989) was added. Tissue was then homogenized in a TissueLyser LT homogenizer (Qiagen #85600) for 5 min at 50 Hz followed by incubation at 95 ºC during 10 min. Protein lysates were briefly spun down and the supernatants were transferred to a new microcentrifuge tube.

Protein extracts were quantified using the Pierce 660nm Protein Assay Kit (Thermo #22662) supplemented with Ionic Detergent Compatibility Reagent (Thermo #22663) in a 96-well plate, according to manufacturer's protocol. Samples were diluted to the same final concentration, mixed with 1x Orange G dye (Sigma #O3756) containing 10% β-mercaptoethanol (Sigma #M3148) and incubated 10 min at 100 ºC before loading. Precast 4-15% TGX protein gels (Bio-Rad) were loaded with 10-20 µg of total protein lysate and run for 1h at 135V. Proteins were transferred to 0.45 µm nitrocellulose membrane (Bio-Rad #1704271) with a Trans-Blot Turbo Transfer system (Bio-Rad) using the pre-determined high molecular weight transfer protocol (10 min, 2.5 A constant). Blocking of the membrane was performed using Intercept (TBS) Blocking Buffer (LI-COR #927-60001) for at least 1h at room temperature. Incubation with primary antibodies (diluted in blocking buffer containing 0.1% Tween-20) was carried out overnight at 4 ºC. Rabbit anti-SYNGAP1 (Cell Signaling Technology #5539S, 1:1000 dilution), rabbit anti-STXBP1 (Munc18-1, Cell Signaling Technology #13414S, 1:1000 dilution) and mouse anti-ATP5F1 (Abcam #ab117991, 1:1000 dilution) were used. Membrane was then rinsed with 1x Tris-buffered saline with 0.1% Tween (TBST) 4 times for 5 min. Incubation with secondary antibodies (diluted in blocking buffer containing 0.1% Tween-20) was performed at room temperature for 1h. For STXBP1 blots, IRDye 680RD anti-rabbit (LI-COR #926-68073, 1:10,000 dilution) and IRDye 800CW anti-mouse (LI-COR #926-32212, 1:10,000 dilution) were used. For SYNGAP1 blots, IRDye 800CW anti-rabbit (LI-COR #926-32213) and IRDye 680RD anti-mouse (LI-COR #926-68072) were used. Membrane was rinsed again with 1x TBST 4 times for 5 min and imaged on Odyssey Imager (LI-COR) using a resolution of 169 µm.

Western blot quantifications were normalized to ATP5F1 according to LI-COR's Housekeeping Protein Normalization Protocol. A standard curve was included in each blot to ensure the linearity of the assay.

Statistical analyses

Measurements were taken from distinct samples. The number of samples is stated explicitly in the figure and represented as individual data points for bar graphs. Kaplan–Meier survival curves were used to represent the survivability of the different model mice and the Mantel–Cox (Log-rank) test was used to statistically compare the overall survival between groups. Statistical significance was defined as $p < 0.05$. Data plots and statistical analyses were performed in GraphPad Prism 10.1 software. Individual statistical tests applied to each data set are given in the respective figure legends. Data represented as mean values ± SEM.

Table 1. qPCR primer-probe sets used in this study.

Copy number variation/Genotyping assay				
Name	**Forward primer**	**Reverse primer**	**Probe**	**Assay ID**
Mouse_Syngap1_gDNA	GCAGTTGTGTGTTCATCTGTTC	CAGCCCTCATTCACCTCTTT	TGAGCATCAGTACGGGCAAAGCAT	NA
Human_SYNGAP1_gDNA	CCCTGACCTCTCTTCTGATAG	CTCTGGCCTAGGGTAAATG	CTGTTCCTGTCCAACCATCACTG	NA
Mouse_Stxbp1_gDNA	TCAAGAGAGTTGGTGACAGA	CCCTTTGCCCCTTCAGTTTC	TTTGAAAGGAATTCTAGGGGATCG	NA
Human_STXBP1_gDNA	CAGGATCTCAGTGTGAAGCTAAG	GGACAGGGCTTACAATCCTAAA	TCTGGTTTGGTGTGACAGGCTCAG	NA
Mouse_Tert_gDNA	GAGACAATGGGTGGCAGTAA	GCTTGGAGTCAGAGACCATAAG	ATGCAGTCCGTGGTTGGATGAGTT	NA
RT-qPCR				
Name	**Forward primer**	**Reverse primer**	**Probe**	**Assay ID**
Mouse_Syngap1_mRNA	GAGTGAGAAGCGCTTGAGA	TTCTTGGGCTCAGGCAG	CAGCAGCAGGTGGAGAAGGACT	NA
Human_SYNGAP1_mRNA	GCAGAGTGAGAAGAGGCTA	TCCTCCACCAGCATCAG	TCCCAGATCAAGAGCATCATTGGCA	NA
Total_SYNGAP1_mRNA	GCTGGATGAGGATGAGATACAC	GAGCGACCCAAGTGGTATT	AACAAACTGCTGAGACGCAC	NA
Mouse_Stxbp1_mRNA	CGTATCAGTGAGCAGACCTA	GGTAGTGCTTTGTATCCAGC	AGACATTATGGAGGACACTATCGAAGACA	NA
Human_STXBP1_mRNA	CATCAGCGAGCAGACCTA	GGTAGTGTTTGGTGTCAAGT	AGGACATCATGGAGGACACTATTGAGGA	NA
Total_STXBP1_mRNA	ACAAGCACATCGCAGAGG	TTCTTCAGCATCTGGGACAG	AGGAAGTCACCCGGTCTCTGAA	NA
Mouse_Atp5f1_mRNA	Proprietary	Proprietary	Proprietary	Thermo (Mm05814774_g1)

Results

Generation of knock-in *Syngap1* and *Stxbp1* humanized mice

The *Syngap1* and *Stxbp1* humanized mice are two distinct non-conditional KI models in which the mouse *Syngap1* and the mouse *Stxbp1* locus were replaced with the human *SYNGAP1* (**Figure 1A**) and the human *STXBP1* (**Figure 2A**) gene, respectively (see details on mouse engineering in **Materials and Methods**). For both mouse models, we generated hybrid (*Syngap1*$^{Hu/+}$ or *Stxbp1*$^{Hu/+}$), fully humanized (*Syngap1*$^{Hu/Hu}$ or *Stxbp1*$^{Hu/Hu}$) and wild-type littermate (*Syngap1*$^{+/+}$ or *Stxbp1*$^{+/+}$) animals. Using a CNV qPCR assay from gDNA, we confirmed the presence of the human *SYNGAP1* (**Figure 1B**) or *STXBP1* (**Figure 2B**) transgene in the targeted mouse locus in hybrid (1 copy) and fully humanized (2 copies) mice relative to wild-type littermates (0 copies). This assay was subsequently used to routinely genotype the mice. In terms of physical appearance, *Syngap1* model mice were indistinguishable from pure C57BL/6 mice, while *Stxbp1* model mice occasionally presented abnormal tail morphologies (i.e. kinked tails).

Survivability

We conducted a 36-week-long survivability study for both *Syngap1* and *Stxbp1* humanized mouse models including male and female mice with hybrid, fully humanized and wild-type genotypes. Mouse viability was not affected in hybrid nor fully humanized *Syngap1* mice, indicating that both mono- and bi-allelic humanization of the *Syngap1* locus are well tolerated. Our body weight data did not show significant differences on mice growth rate across the different *Syngap1* genotypes (**Figure 1C**). We also evaluated potential deviations of genotype distributions from the expected normal Mendelian inheritance among weaned pups. To do that, we calculated the genotypic ratios from the offspring of *Syngap1* hybrid matings (*Syngap1*$^{Hu/+}$ x *Syngap1*$^{Hu/+}$), which should result in 50% of *Syngap1*$^{Hu/+}$, 25% of *Syngap1*$^{Hu/Hu}$ and 25% of *Syngap1*$^{+/+}$ mice. The observed genotypic ratios for *Syngap1* mice followed normal Mendelian inheritance (**Figure 1D**).

Bi-allelic humanization of the *Stxbp1* gene significantly reduced viability. Male *Stxbp1*$^{Hu/Hu}$ presented an abrupt ~90% mortality rate around 9 weeks of age, while *Stxbp1*$^{Hu/Hu}$ females showed a milder, more stepwise mortality phenotype with a ~30% mortality at 36 weeks (**Figure 2C**). However, these observations were not recapitulated in either male or female *Stxbp1*$^{Hu/+}$ mice that carry only one copy of the human *STXBP1* gene, suggesting that mono-allelic but not bi-allelic humanization is well tolerated (**Figure 2C**). The body weights from male *Stxbp1*$^{Hu/Hu}$ mice were not significantly different from hybrid or wild-type littermates and confirmed the absence of weight loss preceding the death of the animal, discarding growth impairments as a potential cause of death (**Figure 2D**). When evaluating the genotypic distribution from the offspring of *Stxbp1* hybrid matings (*Stxbp1*$^{Hu/+}$ x *Stxbp1*$^{Hu/+}$), we observed an apparent underrepresentation in the number of weaned *Stxbp1*$^{Hu/Hu}$ mice (~15% of the offspring) relative to the expected 25% Mendelian ratio (**Figure 2E**). These data suggest ~40% embryonic lethality in *Stxbp1*$^{Hu/Hu}$ mice.

Molecular characterization

We next characterized the *Syngap1* and *Stxbp1* humanized mouse models at the RNA and protein level with samples isolated from cerebral cortex.

Syngap1$^{Hu/Hu}$ mice expressed only human *SYNGAP1* transcript, while *Syngap1*$^{Hu/+}$ showed a ~50% reduction in human *SYNGAP1* mRNA levels relative to *Syngap1*$^{Hu/Hu}$, as expected (**Figure 1E**, middle panel). Human *SYNGAP1* expression was also inversely correlated with mouse *Syngap1* expression, confirming successful humanization of the locus (**Figure 1E**, left panel). Using a cross-reactive qPCR assay that detects both mouse and human *SYNGAP1* transcripts, we observed an ~1.4x increase in the abundance of total *SYNGAP1* mRNA in both *Syngap1*$^{Hu/+}$ and *Syngap1*$^{Hu/Hu}$ mice (**Figure 1E**, right panel). These data indicate *SYNGAP1* is efficiently transcribed following humanization of its genomic locus.

We performed western blotting using a SYNGAP1 antibody raised against a fully conserved region of the protein surrounding Arg1070 (mouse and human SYNGAP1 are 99% conserved at the amino acid level). *Syngap1*$^{Hu/Hu}$ showed a ~35% increase in total SYNGAP1 protein levels relative to wild-type littermates, with a subtler potential increase in expression with mono-allelic humanization (**Figure 1F**). Together with the augmented total *SYNGAP1* mRNA levels, our data point towards modestly enhanced transcription of

the human *SYNGAP1* gene and/or increased stability of the human *SYNGAP1* mRNA in the mouse cellular context as a plausible explanation for SYNGAP1 protein upregulation in fully humanized mice.

Stxbp1$^{Hu/Hu}$ mice expressed only human *STXBP1* mRNA, concomitant with a lack of expression of the mouse gene, confirming successful humanization (**Figure 2F**, left and middle panels). Our cross-reactive qPCR assay did not detect significant differences in total STXBP1 mRNA levels across the different genotypes (**Figure 2F**, right panel). When assessing STXBP1 protein abundance (100% conservation of STXBP1 amino acid sequence between mouse and human), we observed a ~40% reduction in STXBP1 protein levels in *Stxbp1*$^{Hu/Hu}$ mice relative to wild-type littermates (**Figure 2G**). Surprisingly, the reduction in STXBP1 levels was not human gene dosage-sensitive, since STXBP1 protein abundance was not altered in *Stxbp1*$^{Hu/+}$ mice (**Figure 2G**). The STXBP1 downregulation observed in *Stxbp1*$^{Hu/Hu}$ cannot be explained by a transcriptional regulatory mechanism, since total *STXBP1* mRNA levels were unaffected in these mice. Post-transcriptional dysregulation of the human *STXBP1* mRNA in the murine context may contribute to reduced expression, as could the insertion of additional human genomic elements not naturally present in the mouse genome (such as miR-3911 and a lncRNA encoded in the reverse strand, see Figure 2A). Yet, such dysregulation would be expected to produce an intermediate reduction in protein expression in *Stxbp1*$^{Hu/+}$ mice, which was not observed. This raises the possibility that reduced *STXBP1* expression may be a secondary consequence of an unanticipated, pathogenic phenotype resulting from bi-allelic humanization of this locus. Strategies to mitigate are discussed below.

Discussion

Here we generate and characterize *Syngap1* and *Stxbp1* humanized mouse models to provide a novel platform for therapeutic development in SYNGAP1- and STXBP1-related disorders. For both mouse models, the humanization also includes upstream (promoter and proximal enhancers) and downstream (3'UTR) regulatory regions to enable testing of human-specific therapies targeting these elements.

The *Syngap1* humanized mouse colony can be easily maintained on a *Syngap1*$^{Hu/Hu}$ background and rapidly expanded as needed due to its Mendelian inheritance and normal mouse viability and lifespan. It is worth noting that *Syngap1* humanization also includes the human *SYNGAP1* antisense transcript (*SYNGAP1-AS*), which may modulate *SYNGAP1* expression and thus be a potential therapeutic target that is only available in the humanized animal. Our *SYNGAP1* mRNA and protein data from *Syngap1*$^{Hu/Hu}$ mice shows a modestly higher expression of the human gene in the murine context, but we do not anticipate this small difference in basal levels of SYNGAP1 to confound therapeutic targeting of human *SYNGAP1*. As a next step, these humanized mice can be crossed with currently available haploinsufficiency mouse models (12,14) to generate *Syngap1* humanized haploinsufficient mice (*Syngap1*$^{Hu/-}$), which we have confirmed are viable. This represents an ideal model for phenotypic rescue assessments after therapeutic intervention using human gene-targeted compounds.

In contrast, the *Stxbp1* humanized mice have value but also limitations that need to be addressed to broaden the utility of this model. While the genetic cause for the impaired viability of *Stxbp1*$^{Hu/Hu}$ mice (especially males) is unclear, introducing genetic variability in the strain improves their viability. This is evidenced by the fact that our original *Stxbp1*$^{Hu/Hu}$ animals in a pure C57BL/6J genetic background were not viable until they underwent a one-generation outcross with the BALB/c strain to generate the mouse model characterized in this work. Accordingly, we anticipate that *Stxbp1*$^{Hu/Hu}$ viability and their Mendelian ratios can be further improved through additional outcrossing to BALB/c or other strains. This reduced viability and reduced STXBP1 expression in the current model will likely create challenges in generating a humanized haploinsufficient *Stxbp1* mouse model (*Stxbp1*$^{Hu/-}$). The current *Stxbp1*$^{Hu/Hu}$ mice, particularly females, may still prove useful to evaluate target engagement of human-specific therapeutics. Alternatively, *Stxbp1*$^{Hu/+}$ mice exhibit normal viability and levels of STXBP1, and as such may also serve as a useful tool for the research community.

References

1. López-Rivera JA, Pérez-Palma E, Symonds J, Lindy AS, McKnight DA, Leu C, et al. A catalogue of new incidence estimates of monogenic neurodevelopmental disorders caused by de novo variants. Brain [Internet]. 2020 Apr 1 [cited 2024 Aug 1];143(4):1099–105. Available from: https://dx.doi.org/10.1093/brain/awaa051

2. Kovačević J, Maroteaux G, Schut D, Loos M, Dubey M, Pitsch J, et al. Protein instability, haploinsufficiency, and cortical hyper-excitability underlie STXBP1 encephalopathy. Brain. 2018 May 1;141(5):1350–74.

3. Berryer MH, Hamdan FF, Klitten LL, Møller RS, Carmant L, Schwartzentruber J, et al. Mutations in SYNGAP1 Cause Intellectual Disability, Autism, and a Specific Form of Epilepsy by Inducing Haploinsufficiency. Hum Mutat. 2013 Feb;34(2):385–94.

4. Vlaskamp DRM, Shaw BJ, Burgess R, Mei D, Montomoli M, Xie H, et al. SYNGAP1 encephalopathy: A distinctive generalized developmental and epileptic encephalopathy. Neurology [Internet]. 2019 Jan 8 [cited 2023 Nov 27];92(2):E96–107. Available from: https://n.neurology.org/content/92/2/e96

5. Xian J, Parthasarathy S, Ruggiero SM, Balagura G, Fitch E, Helbig K, et al. Assessing the landscape of STXBP1-related disorders in 534 individuals. Brain. 2022 May 1;145(5):1668–83.

6. Stamberger H, Nikanorova M, Willemsen MH, Accorsi P, Angriman M, Baier H, et al. STXBP1 encephalopathy: A neurodevelopmental disorder including epilepsy. Neurology [Internet]. 2016 Mar 8 [cited 2023 Nov 27];86(10):954–62. Available from: https://n.neurology.org/content/86/10/954

7. Yang R, Feng X, Arias-Cavieres A, Mitchell RM, Polo A, Hu K, et al. Upregulation of SYNGAP1 expression in mice and human neurons by redirecting alternative splicing. Neuron [Internet]. 2023 May 17 [cited 2023 Nov 27];111(10):1637-1650.e5. Available from: http://www.cell.com/article/S0896627323001253/fulltext

8. Dawicki-McKenna JM, Felix AJ, Waxman EA, Cheng C, Amado DA, Ranum PT, et al. Mapping PTBP2 binding in human brain identifies SYNGAP1 as a target for therapeutic splice switching. Nature Communications 2023 14:1 [Internet]. 2023 May 6 [cited 2023 Nov 27];14(1):1–20. Available from: https://www.nature.com/articles/s41467-023-38273-3

9. Lim KH, Han Z, Jeon HY, Kach J, Jing E, Weyn-Vanhentenryck S, et al. Antisense oligonucleotide modulation of non-productive alternative splicing upregulates gene expression. Nature Communications 2020 11:1 [Internet]. 2020 Jul 9 [cited 2022 Mar 10];11(1):1–13. Available from: https://www.nature.com/articles/s41467-020-17093-9

10. Cao Y, Liu H, Lu SS, Jones KA, Govind AP, Jeyifous O, et al. RNA-based translation activators for targeted gene upregulation. Nat Commun. 2023 Dec 1;14(1).

11. Torkzaban B, Kawalerski R, Coller J. Development of a Tethered mRNA Amplifier to increase protein expression. Biotechnol J. 2022 Oct 1;17(10).

12. Kim JH, Lee HK, Takamiya K, Huganir RL. The role of synaptic GTPase-activating protein in neuronal development and synaptic plasticity. J Neurosci [Internet]. 2003 Feb 15 [cited 2023 Nov 28];23(4):1119–24. Available from: https://pubmed.ncbi.nlm.nih.gov/12598599/

13. Verhage M, Maia AS, Plomp JJ, Brussaard AB, Heeroma JH, Vermeer H, et al. Synaptic assembly of the brain in the absence of neurotransmitter secretion. Science [Internet]. 2000 Feb 4 [cited 2023 Nov 28];287(5454):864–9. Available from: https://pubmed.ncbi.nlm.nih.gov/10657302/

14. Araki Y, Gerber EE, Rajkovich KE, Hong I, Johnson RC, Lee HK, et al. Mouse models of SYNGAP1-related intellectual disability. Proc Natl Acad Sci U S A [Internet]. 2023 Sep 12 [cited 2024 Jul 30];120(37):e2308891120. Available from: https://www.pnas.org/doi/abs/10.1073/pnas.2308891120

Figure legends

Figure 1. Characterization of the *Syngap1* humanized mouse model. (**A**) Cartoon depicting the *Syngap1* locus after humanization. FRT and F3 are two heterotypic recognition sequences used for FLP-mediated neomycin and hygromycin cassette removal. The human *SYNGAP1* transgene is flanked with loxP sites. 5' regulatory region indicates promoter and proximal enhancers. (**B**) qPCR from gDNA of wild-type (+/+), hybrid (Hu/+) and fully humanized (Hu/Hu) *Syngap1* mice. *Tert* was used as endogenous control. (**C**) Body weights of *Syngap1* model mice. (**D**) Genotypic ratios from the offspring of *Syngap1*$^{Hu/+}$ x *Syngap1*$^{Hu/+}$ breedings. Cartoon was created with BioRender. (**E**) RT-qPCR from cerebral cortex tissue of 9-week-old *Syngap1* model mice. *Atp5f1* mRNA was used as endogenous control. (**F**) SYNGAP1 western blot from samples in (**E**). ATP5F1 was used as endogenous control. (**B**, **C**, **E** and **F**) Data are represented as mean values ± SEM. Data points represent independent biological replicates. (**E** and **F**) White and gray data points indicate females and males, respectively. (**B, E** and **F**) One-way ANOVA with Dunnett's multiple comparison test vs. wild-type (+/+). (**C**) 2-way ANOVA with Dunnett's multiple comparison test vs. wild-type (+/+) (**D**) Chi-square test (df = 2, n = 45, p = 0.9048). *SYNGAP1-AS*, *SYNGAP1* antisense transcript. FC, fold change. ns, non-statistically significant.

Figure 2. Characterization of the *Stxbp1* humanized mouse model. (A) Cartoon depicting the *Stxbp1* locus after humanization. FRT and F3 are two heterotypic recognition sequences used for FLP-mediated neomycin and hygromycin cassette removal. The human *STXBP1* transgene is flanked with loxP sites. 5' regulatory region indicates promoter and proximal enhancers. (**B**) qPCR from gDNA of wild-type (+/+), hybrid (Hu/+) and fully humanized (Hu/Hu) *Stxbp1* model mice. *Tert* was used as endogenous control. (**C**) Kaplan-Meier survival curves of *Stxbp1*$^{Hu/+}$ and *Stxbp1*$^{Hu/Hu}$ mice. (**D**) Body weights of *Stxbp1* model mice. Red arrow indicates the last data available for male *Stxbp1*$^{Hu/Hu}$. (**E**) Genotypic ratios from the offspring of *Stxbp1*$^{Hu/+}$ x *Stxbp1*$^{Hu/+}$ breedings. Cartoon was created with BioRender. (**F**) RT-qPCR from cerebral cortex tissue of 8-week-old *Stxbp1* model mice. *Atp5f1* mRNA was used as endogenous control. (**G**) STXBP1 western blot from samples in (**F**). ATP5F1 was used as endogenous control. (**B**, **D**, **F** and **G**) Data are represented as mean values ± SEM. Data points represent independent biological replicates. (**F** and **G**) White and gray data points indicate females and males, respectively. (**B, F** and **G**) One-way ANOVA with Dunnett's multiple comparison test vs. wild-type (+/+). (**C**) Mantel-Cox test. (**D**) 2-way ANOVA with Dunnett's multiple comparison test vs. wild-type (+/+). (**E**) Chi-square test (df = 2, n = 94, p = 0.0503). FC, fold change. ns, non-statistically significant.

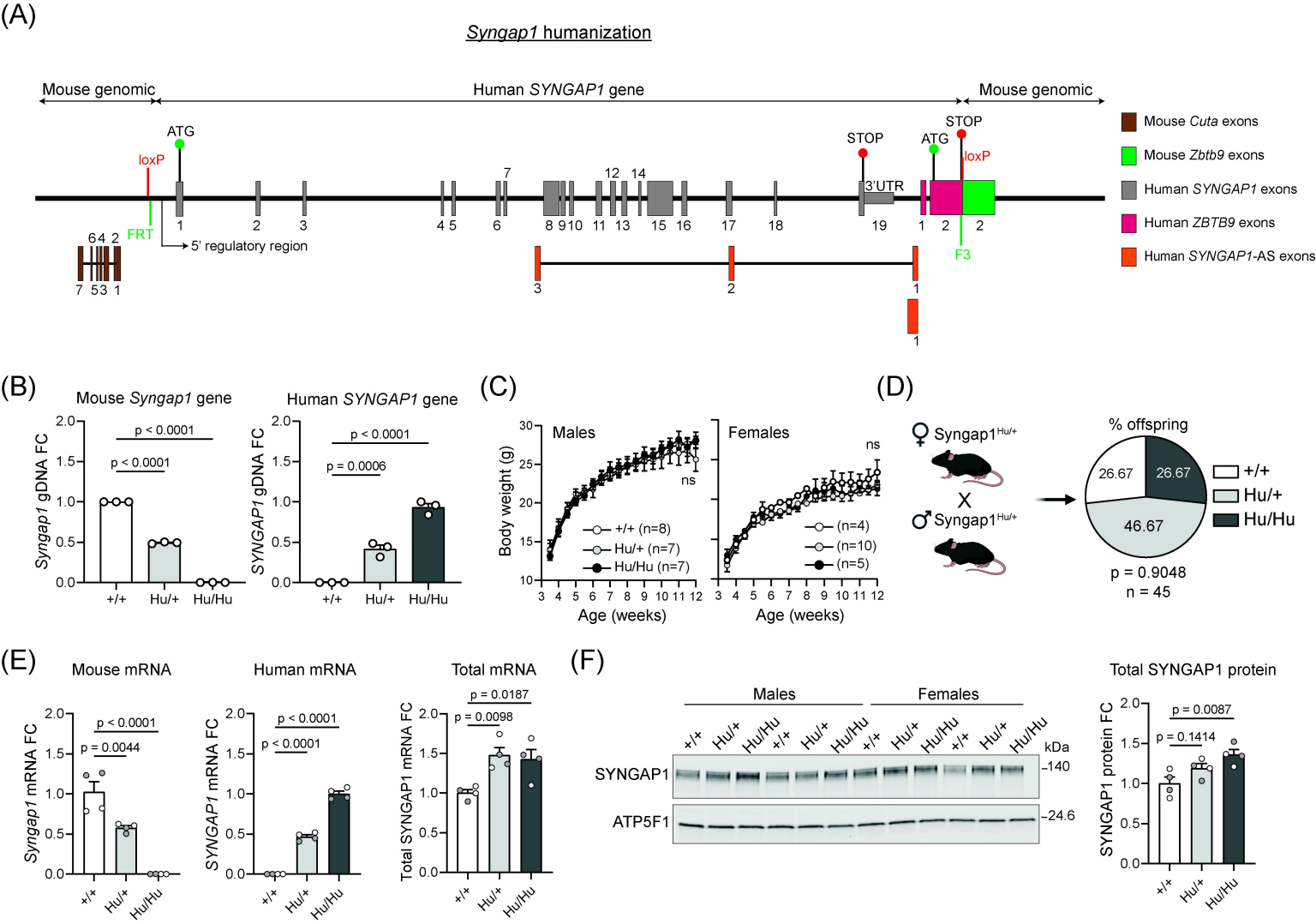
(A)
Syngap1 humanization
Mouse genomic
Human SYNGAP1 gene
Mouse genomic
ATG
loxP
FRT
5' regulatory region
STOP
3'UTR
STOP
ATG
loxP
F3
Mouse Cuta exons
Mouse Zbtb9 exons
Human SYNGAP1 exons
Human ZBTB9 exons
Human SYNGAP1-AS exons
(B)
Mouse Syngap1 gene
Human SYNGAP1 gene
Syngap1 gDNA FC
SYNGAP1 gDNA FC
p < 0.0001
p < 0.0001
p < 0.0001
p = 0.0006
+/+
Hu/+
Hu/Hu
(C)
Males
Females
Body weight (g)
+/+ (n=8)
Hu/+ (n=7)
Hu/Hu (n=7)
(n=4)
(n=10)
(n=5)
ns
ns
Age (weeks)
Age (weeks)
(D)
Syngap1Hu/+
X
Syngap1Hu/+
% offspring
26.67
26.67
46.67
+/+
Hu/+
Hu/Hu
p = 0.9048
n = 45
(E)
Mouse mRNA
Human mRNA
Total mRNA
Syngap1 mRNA FC
SYNGAP1 mRNA FC
Total SYNGAP1 mRNA FC
p < 0.0001
p = 0.0044
p < 0.0001
p < 0.0001
p = 0.0187
p = 0.0098
+/+
Hu/+
Hu/Hu
(F)
Males
Females
+/+
Hu/+
Hu/Hu
kDa
SYNGAP1
-140
ATP5F1
-24.6
Total SYNGAP1 protein
SYNGAP1 protein FC
p = 0.0087
p = 0.1414

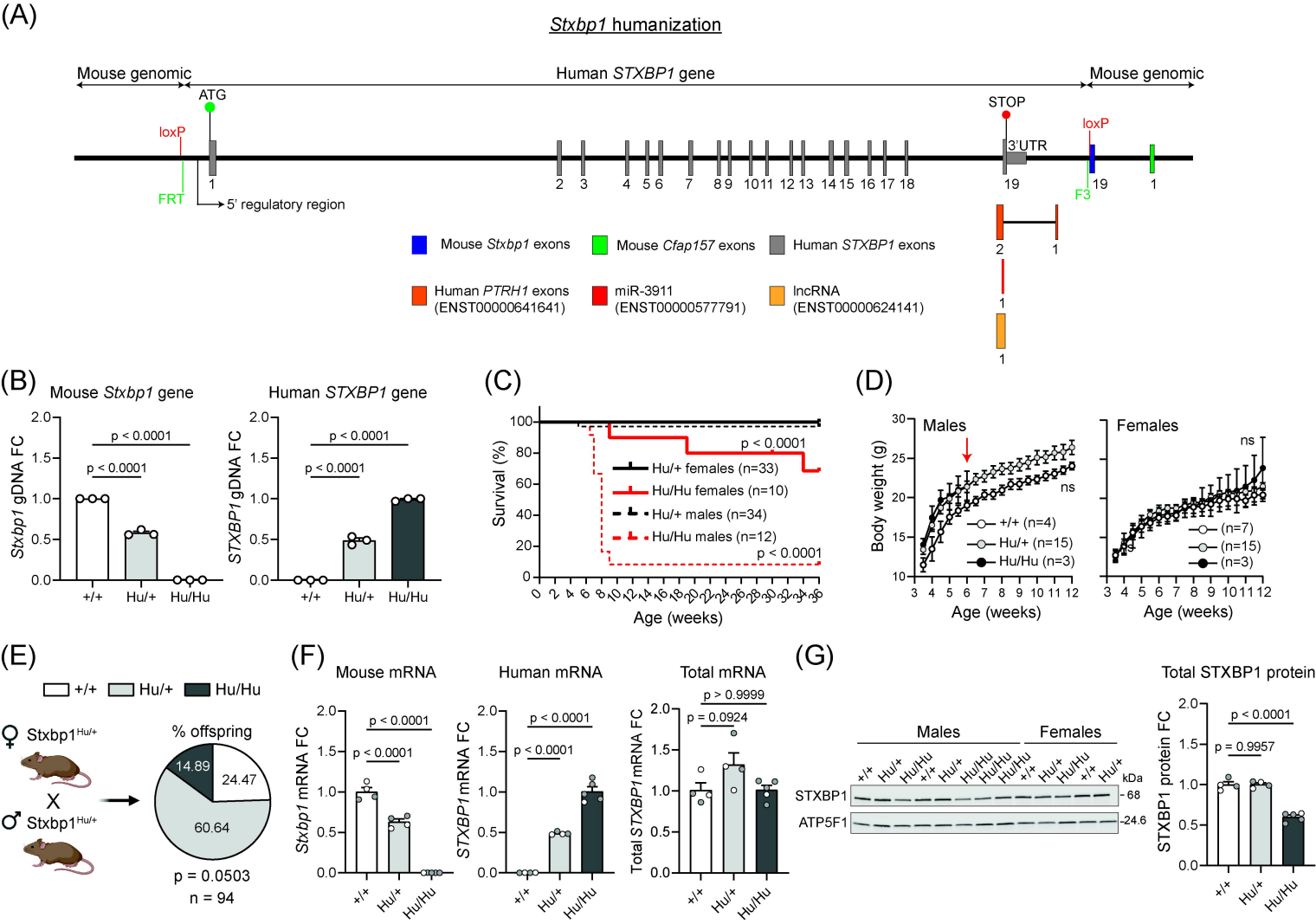
(A)
Stxbp1 humanization
Mouse genomic
Human STXBP1 gene
Mouse genomic
ATG
STOP
loxP
3'UTR
loxP
FRT
F3
5' regulatory region
Mouse Stxbp1 exons
Mouse Cfap157 exons
Human STXBP1 exons
Human PTRH1 exons (ENST00000641641)
miR-3911 (ENST00000577791)
lncRNA (ENST00000624141)
(B)
Mouse Stxbp1 gene
Human STXBP1 gene
Stxbp1 gDNA FC
STXBP1 gDNA FC
p < 0.0001
+/+
Hu/+
Hu/Hu
(C)
Survival (%)
Hu/+ females (n=33)
Hu/Hu females (n=10)
Hu/+ males (n=34)
Hu/Hu males (n=12)
p < 0.0001
Age (weeks)
(D)
Males
Females
Body weight (g)
+/+ (n=4)
Hu/+ (n=15)
Hu/Hu (n=3)
(n=7)
(n=15)
(n=3)
ns
Age (weeks)
(E)
+/+
Hu/+
Hu/Hu
♀ Stxbp1 Hu/+
X
♂ Stxbp1 Hu/+
% offspring
14.89
24.47
60.64
p = 0.0503
n = 94
(F)
Mouse mRNA
Human mRNA
Total mRNA
Stxbp1 mRNA FC
STXBP1 mRNA FC
Total STXBP1 mRNA FC
p < 0.0001
p > 0.9999
p = 0.0924
(G)
Males
Females
STXBP1
ATP5F1
kDa
68
24.6
Total STXBP1 protein
STXBP1 protein FC
p < 0.0001
p = 0.9957